Performance Analysis of Cellular Networks with D2D communication Based on Queuing Theory Model

Jianfang Xin[1,2], Qi Zhu[1*], Guangjun Liang[1,2], Tiaojiao Zhang[1]and Su Zhao[1]
[1] College of Telecommunications and Information Engineering, Nanjing University of Posts and Telecommunications, Nanjing, 210003, China [e-mail: xinjfang@163.com, zhuqi@njupt.edu.cn, 13372266771@163.com, zhaosu@njupt.edu.cn]
[2] electrical engineering School, Anhui Polytechnic University, Wuhu, 241000, China
[e-mail: xinjfang@163.com, lianggjun@ahpu.edu.cn]
*Corresponding author: Qi Zhu

Received August 9, 2017; revised October 12, 2017; revised December 10, 2017; accepted January 15, 2018; published June 30, 2018

Abstract

In this paper, we develop a spatiotemporal model to analysis of cellular user in underlay D2D communication by using stochastic geometry and queuing theory. Firstly, by exploring stochastic geometry to model the user locations, we derive the probability that the SINR of cellular user in a predefined interval, which constrains the corresponding transmission rate of cellular user. Secondly, in contrast to the previous studies with full traffic models, we employ queueing theory to evaluate the performance parameters of dynamic traffic model and formulate the cellular user transmission mechanism as a M/G/1 queuing model. In the derivation, Embedded Markov chain is introduced to depict the stationary distribution of cellular user queue status. Thirdly, the expressions of performance metrics in terms of mean queue length, mean throughput, mean delay and mean dropping probability are obtained, respectively. Simulation results show the validity and rationality of the theoretical analysis under different channel conditions.

Keywords: Device-to-Device (D2D) communication; stochastic geometry; M/G/1 queuing model; Markov chain

The work is supported by Natural Science Foundation of China (61571234,61401225), National Program on Key Basic Research Project(No.2013CB329005), Jiangsu Provincial National Science Foundation(BK20140894), the Key Projects of Support Program for Outstanding Youth Talent of Universities in Anhui Province (gxyqZD2016123) and Youth Foundation of Anhui Polytechnic University(2014YQ40), Anhui higher education promotion plan general project (KZ00215021, KZ00215022)

http://doi.org/10.3837/tiis.2018.06.002 **ISSN : 1976-7277**

1. Introduction

Enabling device-to-device (D2D) communication in cellular networks permits mobile terminals communication directly with each other in authorized spectrum band under the control of the Base Station (BS). In contrast with traditional cellular system, this communication mode enhances spectral efficiency and extends cellular coverage. Since D2D communication possesses strong flexibility and expansibility in communication mode and network structure, it is foreseen as one of key technologies for 5G wireless communication [1].

D2D-enabled cellular networks is classified by underlay and overlay on the basis of D2D users reusing non-orthogonal or orthogonal time/frequency cellular resources. Underlay in-band D2D communication introduces interference inevitably between D2D users and cellular users. Therefore, how to deal with the interference is an important research field [2-4]. Generally speaking, joint of resource allocation and dynamic power control algorithms are proposed to mitigate interference from D2D users to cellular users(CUs) [5-7]. For example, [7] proposes a joint mode selection and resource allocation scheme to maximize the system throughput while guaranteeing Quality of Service (QoS) of both D2D and cellular links. Further, [8] address to maximize the sum of all users logarithmic utility functions by considering both QoS requirement and users' fairness with co-channel interference.

However, the system models of above-mentioned discussed in [5-8] are concentrate on signal-cell scenario and not consider inter-cell interference. Since the users in cell boundary are inevitably suffered interference from the adjacent cell, it is crucial to model D2D-enabled cellular networks in multiple cells. Stochastic Geometry provide a power mathematical method to model Large Scale Network and the mobile user’s positions are modeled as a homogeneous Poisson point process instead of deterministic distribution on a regular grid. The remarkably simple formulas of coverage probability and mean achievable rate are derived with quantifying interference level.

In the last few years, stochastic geometry [9] has been widely used to model and analyze ad-hoc networks, multi-tier cellular networks, as well as hybrid networks [10-11]. In [12], stochastic geometry is adapted to model large-scale network for D2D communication underlying cellular network. A joint channel assignment and power allocation algorithm is proposed to deal with the intra-cell and inter-cell interference management problems. [13] focuses on the intra-cell interference and propose a D2D mode selection scheme to manage it inside a finite cellular network region. The average number of successful D2D transmissions and the spectrum reuse ratio are evaluated the overall quality of underlay D2D communication are analyzed in Nakagami-m fading channels. [14] investigates a general analytical framework to conduct for D2D overlay and underlay scenarios and apply the Poisson point processes to model the spatial distribution of UEs. Then, average ergodic rate is derived to optimize spectrum sharing parameters. Using the Poisson point processes (PPPs) theory in [15], the authors develop a tractable analytical framework to model the effect of flexible mode selection scheme. It is worth to notice, [10-15] are assuming that there are infinite data in the user buffer waiting to be transmitted. Nevertheless, real time data streams are random generated in cellular networks in the actual communication systems. However, the users in Stochastic Geometry models are usually assumed to be saturation with infinite backlogs. To be specific, some key parameters such as delay and dropping probability are greatly affected by the data arrival and queue backlog state.

Queueing theory has been widely used in Vehicular Ad-hoc Networks [16], Wireless Sensor Networks [17] and cooperative cognitive radio network [18-19]. Queueing theory plays a major role in establishing dynamic traffic model to evaluate network performance. [20] studies the performance of D2D communications with dynamic interference and models the system behavior as a coupled processor queuing model. Its steady state distribution is derived approximately by using Stochastic Petri Nets. However, the assumption of treating SINR as the virtual SNR and follow exponential distribution is unsuitable in practice. In this paper, the distribution of SINR is derived by modelling the user locations as Poisson point process. Obviously, the scenario is much more accurate for the heterogeneous area. In [21], the authors investigate the performance of resource allocation schemes in D2D communications by formulating a queuing mode under resource allocation strategy. [20-21] are concerned about D2D dedicated mode which has lower frequency efficiency than D2D reuse mode which is adapted in this paper.

While taking into account of the interference and channel fading in heterogeneous network, data transmission process is relevant to the transmission signal-to-interference-plus-noise ratio (SINR) of cellular user. Therefore, we assume independent and irrelevant of SINR in each time slot. The transmissions rates of the queue departure process are determined by SINR are varying slot by slot. We formulate a M/G/1 queueing model for each cellular user, where M stands for Passion arrival process and G stands for traffic sending process which follows general distribution which account for the interference from inter-cell and intra-cell. Then, because of the generality of server time, a two-dimensional Markov process is constructed to capture the time-varying service rates, which essentially increase the difficulty of solution. We construct embedded Markov chain at the time of data packets departure from the queue, which simplify difficulty for analyzing M/G/1queueing model.

In this paper, a spatiotemporal model is modeled to analysis of cellular user in underlay D2D communication by using stochastic geometry and queueing theory, while the interference to cellular link come from inter-cell and intra-cell. We adapt the stochastic geometry to model the user locations as Poisson point process and apply channel inversion for cellular user uplink power control. The probability of cellular user instantaneous SINR lie in a certain value interval is derived, which is corresponding to the probability of transmission rate of typical CU. Further, we describe the queueing analysis of the typical CU with a dynamic traffic model which consider adaptive transmission rate vary with SINR value. Then, the cellular user transmission mechanism is modeled as a M/G/1 queuing model and Embedded Markov chain is explored to compute its stationary distribution. The expressions of system performance are derived such as mean queue length, mean throughput, mean delay and mean dropping probability for CU queue.

The main contributions of this paper are summarized as follows.

1) We develop a spatiotemporal model to analysis of cellular user in underlay D2D communication by using stochastic geometry and queueing theory. Stochastic geometry is used to derive the probability of cellular user instantaneous SINR lying in a certain value interval. It is assumed that spatial distribution of users follow homogeneous Poisson Point Process and channel inversion power control that guarantees the minimum required received power of BS.

2) A new transmission strategy of adaptive transmission rate provides multiple rates on account of interference conditions. Since the probability of SINR lies in some region corresponding to the probability of multiple transmission rates, a M/G/1 queueing model is formulated to capture the behavior of the CU with time-varying channel condition and finite

capacity buffer. We take in account of the influence of overflow to the system performance and data transmission rate is determined by SINR value.

3)In order to analyze the CU queue length state of the packets in the buffer, we construct a Embedded Markov chain to compute its stationary distribution. Finally, the expressions of performance metrics in terms of mean queue length, mean throughput, mean delay and mean dropping probability are obtained.

The remaining of this paper is organized as follows. In section II, we describe the system model and a series of assumptions. The M/G/1 Queueing Model is solved by Embedded Markov chain in Section III, as well as the performance parameters of throughput, delay and packet drop rate for the queue of cellular user are derived. In Section IV, both the analysis and the simulation results are proposed to compare the theoretical and the simulated value. Section V gives a conclusion for this paper.

2. System Model

In this section we give the system model and system parameters that will be used in subsequent parts of this paper. We consider a D2D underlying cellular network in which D2D links share the uplink cellular spectrum. Note that D2D communication could reuse the downlink channel of the cellular network, but downlink reuse leads to more traffic congestion [13]. As shown in **Fig. 1**, Base Stations are arranged according to a hexagonal grid and the size is denoted by $\frac{1}{\lambda_B}$ where λ_B is regarded as the BS density per unit area. For the convenience of analysis, we approximate the coverage region to a disk A centered by BS with radius $R=\frac{1}{\sqrt{\pi\lambda_B}}$. We further assume that the location of cellular users follows the Poisson Point Process, denoted as Φ_C with density λ_C. In order to analyze conveniently, we assume that the fully loaded cellular network scenario in which each uplink sub-channel is allocated to only one cellular user (CU) in each cell and spectrum-sharing exist among cells. Cellular users are uniformly distributed in one cell and we define the distance from the typical CU to its serving base station as $r, r\in(0,R)$. The probability density function of r is $\frac{2r}{R^2}$.

Furthermore, we assume that each D2D transmitter has an intended receiver with a fixed communication distance. The locations of D2D transmitters are assumed to follow a 2-D homogeneous PPP distribution Φ_D with density λ_D. Because of only one CU uplink sub-channel could be reused by D2Ds in each cell, the density of CU λ_C is the same as the BS density λ_B. Furthermore, the interferences of CU link are from multiple co-channel D2D transmitters within a cell by assuming $\lambda_D > \lambda_B$. We assume each node has one antenna.

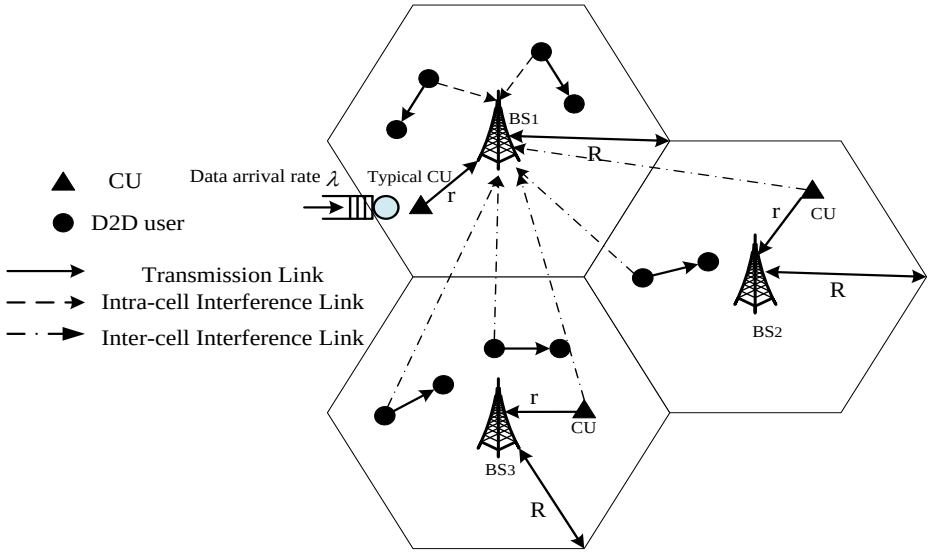

Fig. 1. System model of D2D communications underlaying cellular network in multi-cell, which consider the top cell as a typical cell and a typical CU with dynamic data flow in the cell. λ is denoted as average arrival rate of Poisson process.

We consider the path-loss plus block fading channel model, in which the received signal power decays $d^{-\alpha}$ in the distance d away from transmitter, where $\alpha > 2$ is the path-loss exponent. Furthermore, Rayleigh fading is assumed to model the small-scale fading between the transmitter and receiver, which follow exponentially distribute with unit mean. We assume that uplink power control is employed to maintain the received power of BS from cellular user equal to a certain threshold ρ_{BS}. Then the transmit power of cellular use is $\rho_{BS} r_{\kappa,BS}^{\alpha_C}$, where $r_{\kappa,BS}$ is the distance between CU κ and its server BS and α_C is denoted as pass-loss exponent of the cellular link.

Under the description of system model aforementioned, there are two kinds of interference for a cellular user, which come from outside and inside of the cell. The first category is intra-cell interference caused by the shared frequency spectrum between a cellular user and D2D users. The second category is inter-cell interference which come from D2D users and CUs in other cells with non-orthogonal radio access scheme. Under this system model, the SINR experienced at the BS associated with the typical CU κ can be written as

$$\gamma = \frac{g_{\kappa,BS}\rho_{BS}}{I_{agg}^{C} + I_{agg}^{D} + \delta^2} = \frac{g_{\kappa,BS}\rho_{BS}}{\sum_{i\in\Phi_C\setminus\{\kappa\}} \rho_{BS} r_{\kappa,BS}^{\alpha_C} d_{i,BS}^{-\alpha_C} g_{i,BS} + \sum_{j\in\Phi_D} P_d g_{j,BS} d_{j,BS}^{-\alpha_D} + \delta^2} \tag{1}$$

Where $g_{\kappa,BS}$ is the fading power gain between CU κ and the BS. I_{agg}^{C} and I_{agg}^{D} denote the aggregate interference from CUs in the other cells and interference from D2D users. Considering the cellular links and the D2D links may have different propagation channels, α_C and α_D are denoted as pass-loss exponent of the cellular link and the D2D link and the

interference links fading power gain as $g_{i,BS}$, $g_{j,BS}$, which are assumed to be the independent identically distributed. $d_{i,BS}^{-\alpha_C}$ and $d_{j,BS}^{-\alpha_D}$ are denoted as the distance of CU i and D2D user j to the service BS of CU κ respectively. P_d is D2D transmitter power and the noise power is assumed to be δ^2. The uplink coverage probability of the typical CU is expressed as

$$\begin{aligned} P\left[\gamma > \xi_0^{th}\right] &= E_r\left[P\left[\gamma > \xi_0^{th} \middle| r\right]\right] \\ &= \int_0^R P\left[\gamma > \xi_0^{th} \middle| r\right] f_r(r)\, dr \\ &= \int_0^R P\left[\frac{g_{\kappa,BS}\rho_{BS}}{I_{agg}^C + I_{agg}^D + \delta^2} > \xi_0^{th} \middle| r\right] \frac{2r}{R^2} dr \\ &= \int_0^R \frac{2}{R^2} P\left[g_{\kappa,BS} > \frac{\xi_0^{th}}{\rho_{BS}}\left(I_{agg}^C + I_{agg}^D + \delta^2\right)\right] r dr \end{aligned} \tag{2}$$

Because of $g_{\kappa,BS} \sim \exp(1)$, by following the same derivation given in [9], the coverage probability is expressed as

$$\begin{aligned} P\left[g_{\kappa,BS} > \frac{\xi_0^{th}}{\rho_{BS}}\left(I_{agg}^C + I_{agg}^D + \delta^2\right) \middle| r\right] &= E_{I_{agg}^C,\ I_{agg}^D}\left[P\left[g_{\kappa,BS} > \frac{\xi_0^{th}}{\rho_{BS}}\left(I_{agg}^C + I_{agg}^D + \delta^2\right) \middle| r, I_{agg}^C,\ I_{agg}^D\right]\right] \\ &= E_{I_{agg}^C,\ I_{agg}^D}\left[\exp\left(-\frac{\xi_0^{th}}{\rho_{BS}}\left(I_{agg}^C + I_{agg}^D + \delta^2\right)\right) \middle| r, I_{agg}^C,\ I_{agg}^D\right] \\ &= e^{-\frac{\xi_0^{th}}{\rho_{BS}}\cdot\delta^2} \cdot \mathcal{L}_{I_{agg}^D}\left(\frac{\xi_0^{th}}{\rho_{BS}}\right) \cdot \mathcal{L}_{I_{agg}^C}\left(\frac{\xi_0^{th}}{\rho_{BS}}\right) \end{aligned} \tag{3}$$

Where $\mathcal{L}_{I_{agg}^D}(s)$ and $\mathcal{L}_{I_{agg}^C}(s)$ are the Laplace transforms of I_{agg}^C and I_{agg}^D. $\mathcal{L}_{I_{agg}^D}(s)$ and $\mathcal{L}_{I_{agg}^C}(s)$ can be expressed as [9]

$$\begin{aligned} \mathcal{L}_{I_{agg}^D}(s) &= E_{I_{agg}^D}\left[e^{-sI_{agg}^D}\right] \\ &= E_{\Phi_D, g_{j,BS}}\left[\exp\left(-s\sum_{i\in\Phi_d} P_d g_{j,BS} d_{j,BS}^{-\alpha_D}\right)\right] \\ &\overset{(i)}{=} E_{\Phi_D}\left[\prod_{j\in\Phi_D} E_{g_d}\left[\exp\left(-sP_d g_d d_{j,BS}^{-\alpha_D}\right)\right]\right] \\ &\overset{(ii)}{=} \exp\left(-2\pi\lambda_d \int_0^\infty \left(1 - E_{g_d}\left[\exp\left(-sg_d P_d v^{-\alpha_D}\right)\right]\right) v\, dv\right) \\ &= \exp\left(-2\pi\lambda_d \int_0^\infty \left(1 - E_{g_d}\left[\frac{1}{1+sP_d v^{-\alpha_D}}\right]\right) v\, dv\right) \end{aligned} \tag{4}$$

Where (i) is true based on the i.i.d. distribution of g_d and (ii) is from the probability generating functional (PGFL) of the PPP. The last equality is due to $g_d \sim \exp(1)$.

$$\begin{aligned}\mathcal{L}_{I_{agg}^C}(s) &= E_{I_{agg}^C}\left[e^{-sI_{agg}^C}\right] \\ &= E_{\Phi_C, g_{i,BS}}\left[\exp\left(-s\sum_{i\in\Phi_C\setminus\{\kappa\}}\rho_{BS}r_{\kappa,BS}^{\alpha_C}d_{i,BS}^{-\alpha_C}g_{i,BS}\right)\right] \\ &= E_{\Phi_C}\left[\prod_{i\in\Phi_C\setminus\{\kappa\}}E_{g_c}\left[\exp\left(-s\rho_{BS}r_{\kappa,BS}^{\alpha_C}d_{i,BS}^{-\alpha_C}g_c\right)\right]\right] \\ &= \exp\left(-2\pi\lambda_c\int_R^\infty\left(1-E_{g_c}\left[\exp\left(-s\rho_{BS}r_{\kappa,BS}^{\alpha_C}d_{i,BS}^{-\alpha_C}g_c\right)\right]\right)vdv\right) \\ &= \exp\left(-2\pi\lambda_c\int_R^\infty\left(1-E_{g_c}\left[\frac{1}{1+s\rho_{BS}r_{\kappa,BS}^{\alpha_C}d_{i,BS}^{-\alpha_C}g_c}\right]\right)vdv\right)\end{aligned} \tag{5}$$

The derivation of $\mathcal{L}_{I_{agg}^C}(s)$ is mostly the same as $\mathcal{L}_{I_{agg}^D}(s)$ except the scope of integral of variable v which denotes the distance between cellular users in other cells and the server BS of typical CU. By substituting (3)-(5) back to (2), the close form expression of the uplink CU coverage probability is obtained, which shows that establishing a communications link between CU and the base station need meet the lower bound of SINR.

With the same assumption in [19-20], the received SINR remain constant value within a slot time under the block-fading channel. We assume that the CU sends packets with different transmission rates that vary with the instantaneous SINR. The selection of data rate is by partitioning the value space of SINR into non-overlapping consecutive intervals $\left\{\xi_k^{th},\xi_{k+1}^{th}\right\}_{k=0}^{k=M}$, where M is the space of SINR value intervals. The set of corresponding transmission rate is denoted as $\chi_i, i\in(0,M)$.

When $\gamma<\xi_0^{th}$, due to the meaning of coverage probability, the transmission link cannot establish communication link with guaranteeing its bit error rate less than a certain threshold. The probability of no data to be sent is $p(\chi_0=0)=1-P\left[SINR>\xi_0^{th}\right]$.

When $\gamma\geq\xi_0^{th}$, we adapt M types of data transmitting rates $\chi_i, i\in(1,M)$ corresponding to M modulation modes. The selection of data rate is by partitioning the value space of SINR into M non-overlapping consecutive intervals and the set of interval is named as $\left\{\xi_k^{th},\xi_{k+1}^{th}\right\}_{k=0}^{k=M}$. If the instantaneous SINR value is within a certain interval $\gamma\in\left(\xi_k^{th},\ \xi_{k+1}^{th}\right); k\in[1,M-1]$, the fixed transmission rate is chosen by the MQAM modulation technique of the IEEE 802.11a standards [22]. Adaptive modulation is efficient to enhance spectral efficiency in fading channels and ensure the packet error rate above the target BER. We assume BS obtains perfect channel state information (CSI) and the chosen modulation mode is fed back to the CU without error. Based on (4) and (5), we can get the

probability of sending data with rate χ_k as follow.

$$\begin{aligned} p(\chi_k) &= P\left[\xi_k^{th} < \gamma < \xi_{k+1}^{th}\right] \\ &= P\left[\gamma > \xi_k^{th}\right] - P\left[\gamma > \xi_{k+1}^{th}\right] \\ &= \int_0^R \frac{2}{R^2} P\left[g_{\kappa,BS} > \frac{\xi_k^{th}}{\rho_{BS}}\left(I_{agg}^C + I_{agg}^D + \delta^2\right)\right] rdr - \int_0^R \frac{2}{R^2} P\left[g_{\kappa,BS} > \frac{\xi_{k+1}^{th}}{\rho_{BS}}\left(I_{agg}^C + I_{agg}^D + \delta^2\right)\right] rdr \\ &= \int_0^R \frac{2e^{-\frac{\xi_k^{th}}{\rho_{BS}}\cdot\delta^2}}{R^2} \cdot \mathcal{L}_{I_{agg}^D}\left(\frac{\xi_k^{th}}{\rho_{BS}}\right) \cdot \mathcal{L}_{I_{agg}^C}\left(\frac{\xi_k^{th}}{\rho_{BS}}\right) rdr - \int_0^R \frac{2e^{-\frac{\xi_{k+1}^{th}}{\rho_{BS}}\cdot\delta^2}}{R^2} \cdot \mathcal{L}_{I_{agg}^D}\left(\frac{\xi_{k+1}^{th}}{\rho_{BS}}\right) \cdot \mathcal{L}_{I_{agg}^C}\left(\frac{\xi_{k+1}^{th}}{\rho_{BS}}\right) rdr \end{aligned} \tag{6}$$

When $\gamma > \xi_M^{th}$, the probability of the sending rate χ_M is obtained by $p(\chi_M) = P\left[\gamma > \xi_M^{th}\right]$.

We consider that the instantaneous SINR falls within a certain region corresponding to transmission rate of typical CU. In the next section, the data packets reception and transmission with dynamic data flow is discussed.

3. Queueing Model Formulation and Performance Measures

We describe the queueing analysis of the typical CU with dynamic finite traffic model in this section. It is assumed that the cellular users of other cells and D2Ds have infinite data traffic. We consider the users location follow Poisson point process to obtain the probability of SINR falling within some region, which corresponding to the probability of multiple transmission rates. The data transmission of cellular user is model as an M/G/1 queueing system with a finite buffer $L_{\max}$. The data service request process of the CU obey Poisson distribution with arrival rate λ packets/sec and the service rates corresponding to sending rates vary with CU received instantaneous SINR value. When arrival data packets exceed buffer size, the follow-up data packets are discarded. The probability of arrival a data packets in CU queue as follows

$$P\left(A_{t_n} = a\right) = \begin{cases} e^{-\lambda\Delta t} \cdot \dfrac{\left(\lambda\Delta t\right)^a}{a!}, & if\ a \geq 0 \\ 0, & otherwise \end{cases} \tag{7}$$

Where A_{t_n} denotes the event of arrival a packets in slot t_n and a is the number of arrival packets during Δt which is the transmission slot duration time.

At the beginning of the slot t_n, if queue length of the CU buffer is less than the data packets which allowed to send according to the current channel state, all the data stored in the buffer are all be sent by the end of slot t_n. The new arrival are queue up at the tail of the queue and start to be sent until the next slot t_{n+1}. Otherwise, besides the newly arrival packets in slot t_n, the instantaneous queue length in slot t_{n+1} also contains the remainder after sending in slot t_n.

Let $Q_{t_{n+1}}$ denote the instantaneous queue length of CU at the beginning of slot t_{n+1} and its expression can be obtained as follows

$$Q_{t_{n+1}} = \min\left(L_{\max}, \max\left(Q_{t_n} - \left\lfloor \frac{\chi_{t_n}\Delta t}{B} \right\rfloor, 0 \right) + A_{t_n} \right) \tag{8}$$

Where Q_{t_n} denote the queue length at the beginning of slot t_n and χ_{t_n} is the data rate in Kbs. The length of data packet is fixed as $Bbits$. Then, the data rate in the duration of slot t_n is expressed as $\frac{\chi_{t_n}\Delta t}{B}$ and $\lfloor \cdot \rfloor$ indicates the maximum integer less than $\cdot$.

We adapt Embedded Markov chain to analysis the packets state of the CU buffer with M/G/1 queuing model. X_n is defined as the number of data packets in the queue, where $n \geq 0$ and its state space $L \in \{0,1,\ldots,L_{\max}\}$. **Fig. 2** shows the state transition probability of M/G/1 queuing system. Seen from **Fig. 2**, let $p_{i,j}$ denotes the transition probability from the queuing length state i to state j of the typical cellular user in the Markov chain.

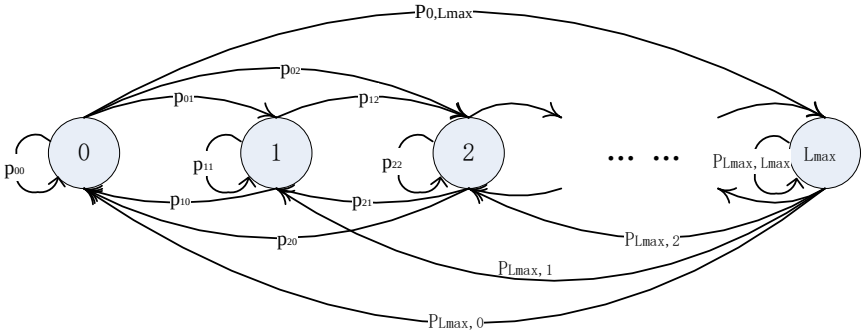

Fig. 2. State transitions of M/G/1 queuing model

$$P\left(Q_{t_{n+1}} = j \middle| Q_{t_n} = i\right) = \begin{cases} P\left(A_{t_n} = j\right) & if\ i = 0 \\ P\left(A_{t_n} = j - i + \left\lfloor \frac{\chi_{t_n}\Delta t}{B} \right\rfloor\right) & if\ 0 < i \leq \left\lfloor \frac{\chi_{t_n}\Delta t}{B} \right\rfloor \\ 0 & if\ i > j + \left\lfloor \frac{\chi_{t_n}\Delta t}{B} \right\rfloor \end{cases} \tag{9}$$

The queue length could be $0,1,2,\ldots,L_{\max}$ in the initial state, the data rate $\chi_k \in (\chi_0, \chi_M)$ that depends on the instantaneous SINR. Then, $p_{i,j}$ can be expressed as

$$p_{i,j} = \sum_{k=0}^{M} p(\chi_k) P\left(Q_{t_{n+1}} = j \middle| Q_{t_n} = i\right) \tag{10}$$

Where $p(\chi_k)$ is denoted as the probability of selecting certain rate as defined below.

For the convenience of description, we assume three data rates in the following transition probability derivation. Without loss of generality, the analytical method is the same as $M+1$ data rates.

Case A: When the original queue is empty, $p_{i,j}$ is the probability of newly arrived j packets during time interval Δt. When the packets number in the queue is less than the minimum transmission rate, the existing packets are transmitted with probability $1-p(\chi_0)$ and j packets are newly arrived with the probability of $e^{-\lambda\Delta t}\frac{(\lambda\Delta t)^i}{j!}$.

$$p_{i,j}=\begin{cases} e^{-\lambda\Delta t}\dfrac{(\lambda\Delta t)^i}{j!}, & i=0 \\ \left(1-p(\chi_0)\right)e^{-\lambda\Delta t}\dfrac{(\lambda\Delta t)^i}{j!}, & 0<i\le\left\lfloor\dfrac{\chi_1\Delta t}{B}\right\rfloor \end{cases} \tag{11}$$

Case B：if $\left\lfloor\frac{\chi_1\Delta t}{B}\right\rfloor<i\le\left\lfloor\frac{\chi_2\Delta t}{B}\right\rfloor$, In this case, when $j<i-\left\lfloor\frac{\chi_1\Delta t}{B}\right\rfloor$, the transmission rate χ_1 cannot send enough packets and the state transition achieves with χ_2 and χ_3 which empty the original packets in the queue. When $j\ge i-\left\lfloor\frac{\chi_1\Delta t}{B}\right\rfloor$, the number of newly arrived data packets is $A=j-i+\left\lfloor\frac{\chi_1\Delta t}{B}\right\rfloor$ with rate χ_1, while the arrival packets $A=j$ with the transmission rate χ_2 and χ_3.

$$p_{i,j}=\begin{cases} p(\chi_2)e^{-\lambda\Delta t}\dfrac{(\lambda\Delta t)^j}{j!}+p(\chi_3)e^{-\lambda\Delta t}\dfrac{(\lambda\Delta t)^j}{j!}, & j<i-\left\lfloor\dfrac{\chi_1\Delta t}{B}\right\rfloor \\ p(\chi_1)e^{-\lambda\Delta t}\dfrac{(\lambda\Delta t)^{\left(\left\lfloor\frac{\chi_1\Delta t}{B}\right\rfloor+(j-i)\right)}}{\left(\left\lfloor\frac{\chi_1\Delta t}{B}\right\rfloor+(j-i)\right)!}+p(\chi_2)e^{-\lambda\Delta t}\dfrac{(\lambda\Delta t)^j}{j!}+p(\chi_3)e^{-\lambda\Delta t}\dfrac{(\lambda\Delta t)^j}{j!}, & j\ge i-\left\lfloor\dfrac{\chi_1\Delta t}{B}\right\rfloor \end{cases} \tag{12}$$

Case C: If $\left\lfloor\frac{\chi_2\Delta t}{B}\right\rfloor<i\le\left\lfloor\frac{\chi_3\Delta t}{B}\right\rfloor$, there are three different transition probability expressions under the condition of $\left\lfloor\frac{\chi_2\Delta t}{B}\right\rfloor<i\le\left\lfloor\frac{\chi_3\Delta t}{B}\right\rfloor$.

$$p_{i,j}=\begin{cases} p(\chi_3)e^{-\lambda\Delta t}\dfrac{(\lambda\Delta t)^j}{j!}, & j<i-\left\lfloor\dfrac{\chi_2\Delta t}{B}\right\rfloor \\ p(\chi_2)e^{-\lambda\Delta t}\dfrac{(\lambda\Delta t)^{\left(\left\lfloor\frac{\chi_2\Delta t}{B}\right\rfloor+(j-i)\right)}}{\left(\left\lfloor\dfrac{\chi_2\Delta t}{B}\right\rfloor+(j-i)\right)!}+p(\chi_3)e^{-\lambda\Delta t}\dfrac{(\lambda\Delta t)^j}{j!}, & i-\left\lfloor\dfrac{\chi_2\Delta t}{B}\right\rfloor\le j<i-\left\lfloor\dfrac{\chi_1\Delta t}{B}\right\rfloor \\ e^{-\lambda\Delta t}\sum_{k=1}^{2}p(\chi_k)\dfrac{(\lambda\Delta t)^{\left(\left\lfloor\frac{\chi_k\Delta t}{B}\right\rfloor+(j-i)\right)}}{\left(\left\lfloor\dfrac{\chi_k\Delta t}{B}\right\rfloor+(j-i)\right)!}+p(\chi_3)e^{-\lambda\Delta t}\dfrac{(\lambda\Delta t)^j}{j!}, & j\ge i-\left\lfloor\dfrac{\chi_1\Delta t}{B}\right\rfloor \end{cases} \tag{13}$$

Case D: If $i>\left\lfloor\dfrac{\chi_3\Delta t}{B}\right\rfloor$

$$p_{i,j}=\begin{cases} 0, & j<i-\left\lfloor\dfrac{\chi_3\Delta t}{B}\right\rfloor \\ p(\chi_3)e^{-\lambda\Delta t}\dfrac{(\lambda\Delta t)^{\left(\left\lfloor\frac{\chi_3\Delta t}{B}\right\rfloor+(j-i)\right)}}{\left(\left\lfloor\dfrac{\chi_3\Delta t}{B}\right\rfloor+(j-i)\right)!}, & i-\left\lfloor\dfrac{\chi_3\Delta t}{B}\right\rfloor\le j<i-\left\lfloor\dfrac{\chi_2\Delta t}{B}\right\rfloor \\ e^{-\lambda\Delta t}\sum_{k=1}^{2}p(\chi_k)\dfrac{(\lambda\Delta t)^{\left(\left\lfloor\frac{\chi_k\Delta t}{B}\right\rfloor+(j-i)\right)}}{\left(\left\lfloor\dfrac{\chi_k\Delta t}{B}\right\rfloor+(j-i)\right)!}, & i-\left\lfloor\dfrac{\chi_2\Delta t}{B}\right\rfloor\le j<i-\left\lfloor\dfrac{\chi_1\Delta t}{B}\right\rfloor \\ e^{-\lambda\Delta t}\sum_{k=1}^{3}p(\chi_k)\dfrac{(\lambda\Delta t)^{\left(\left\lfloor\frac{\chi_k\Delta t}{B}\right\rfloor+(j-i)\right)}}{\left(\left\lfloor\dfrac{\chi_k\Delta t}{B}\right\rfloor+(j-i)\right)!}, & j\ge i-\left\lfloor\dfrac{\chi_1\Delta t}{B}\right\rfloor \end{cases} \tag{14}$$

Using the equation (11)~(14),we can obtain $p_{i,j}$ as follow

$$p_{i,j}=\begin{bmatrix} p_{0,0} & p_{0,1} & p_{0,2} & \cdots & \cdots & \cdots & p_{0,L_{\max}} \\ p_{1,0} & p_{1,1} & p_{1,2} & \cdots & \cdots & \cdots & p_{1,L_{\max}} \\ \vdots & \vdots & \ddots & \ddots & \ddots & \ddots & \vdots \\ p_{\left\lfloor \frac{\chi_K \Delta t}{B} \right\rfloor,0} & p_{\left\lfloor \frac{\chi_K \Delta t}{B} \right\rfloor,1} & \ddots & \ddots & \ddots & \ddots & \vdots \\ 0 & p_{\left\lfloor \frac{\chi_K \Delta t}{B} \right\rfloor+1,1} & p_{\left\lfloor \frac{\chi_K \Delta t}{B} \right\rfloor+1,2} & \ddots & \ddots & \ddots & \vdots \\ \vdots & 0 & \ddots & \ddots & \ddots & \ddots & p_{L_{\max}-1,L_{\max}} \\ 0 & 0 & 0 & \ddots & \ddots & \ddots & p_{L_{\max},L_{\max}} \end{bmatrix} \tag{15}$$

We define that the steady state distribution of the queueing model is $\pi=\left(\pi(0),\pi(1),\cdots\pi\left(L_{\max}\right)\right)$. Assuming that there is no data at the initial time, the initial state is $\pi=(1,0,\cdots 0)$. In the light of normalized to the sum of probability, the steady state distribution is solved by the following matrix equation set [24].

$$\pi\mathbf{P}=\pi,\sum_{l\in L}\pi(l)=1 \tag{16}$$

Here, we present the expressions of performance metrics, such as mean queue length, mean throughput, mean delay, and mean dropping probability. The mean queue length is defined as

$$\overline{Queue}=\sum_{l=0}^{L_{\max}} l\pi(l) \tag{17}$$

The mean throughput of the queue can be acquired as

$$\overline{Throughput}=\sum_{k=1}^{3}P(\chi_k)\left\{\sum_{l=1}^{\left\lfloor \frac{\chi_k \Delta t}{B} \right\rfloor} l\pi(l)+\sum_{l=\left\lfloor \frac{\chi_k \Delta t}{B} \right\rfloor+1}^{L_{\max}}\left\lfloor \frac{\chi_k \Delta t}{B} \right\rfloor\pi(l)\right\} \tag{18}$$

Where $\left\{\sum_{l=1}^{\left\lfloor \frac{\chi_k \Delta t}{B} \right\rfloor} l\pi(l)+\sum_{l=\left\lfloor \frac{\chi_k \Delta t}{B} \right\rfloor+1}^{L_{\max}}\left\lfloor \frac{\chi_k \Delta t}{B} \right\rfloor\pi(l)\right\}$ indicates the throughput under the condition of transmission rate χ_k, which contains two cases. When the packets in the queue are less than Maximum transmission capacity $\left\lfloor \frac{\chi_k \Delta t}{B} \right\rfloor$, the sending packets per unit time is the queue length l multiply by its steady state distribution. When $l>\left\lfloor \frac{\chi_k \Delta t}{B} \right\rfloor$, the sending packets per unit time is transmission capacity with rate χ_k multiply by the steady-state distribution of the waiting line size l. The throughput is zero when the queue line is empty.

The mean delay can be expressed according to Little's Law as follow, which is the average time before a packet departure from the queue.

$$\overline{Delay}=\frac{\overline{Queue}}{Throughput}=\frac{\sum_{l=0}^{L_{\max}} l\pi(l)}{\sum_{k=1}^{3}P(\chi_k)\left\{\sum_{l=1}^{\left\lfloor\frac{\chi_k\Delta t}{B}\right\rfloor} l\pi(l)+\sum_{l=\left\lfloor\frac{\chi_k\Delta t}{B}\right\rfloor+1}^{L_{\max}}\left\lfloor\frac{\chi_k\Delta t}{B}\right\rfloor\pi(l)\right\}} \tag{19}$$

We define B_{t_n} as the dropped packets when $Q(t_n)=l$ and the dropping probability caused by overflow which related with average arrival rate and buffer size can be calculated as:

$$\begin{aligned} p_{drop}&=\frac{\sum_{l=0}^{L_{\max}}\sum_{b=0}^{\infty} bP\left(B_{t_n}=b\right)\pi(l)}{\lambda\Delta t} \\ &=\frac{\sum_{l=0}^{L_{\max}}\sum_{b=0}^{\infty} bP\left(A_{t_n}=L_{\max}+b-\max\left(0,l-\frac{\chi_k\Delta t}{B}\right)\right)\pi(l)}{\lambda\Delta t} \end{aligned} \tag{20}$$

Where b denotes the number of dropped packets in slot t_n.

4. Performance Evaluation

In this section, we present the numerical results from simulation and theoretical analysis to validate the accuracy of the proposed analytical model. The CU communication system performances metrics (i.e., mean queue length, mean throughput, mean delay, and mean dropping probability) are impacted by data arrival rates and different path loss factor. It is also presented the impact of users density and buffer size on the mean dropping probability. The system model as described in section 2, Independent and identically distributed Rayleigh fading with unit variance is considered for all links. Most of the D2D literatures have considered $\alpha_C=\alpha_D$ [25-26], which is adapted path-loss exponent value as 3, 3.5, 4. In the simulation setup, the base stations and users are realized in $400km^2$ area and each cellular user is associated with the closed BS. To validate our derived results, the simulation results are carried out by using MATLAB and repeat for over 10,000 iterations. In our simulation major parameters are listed in **Table 1**.

Table 1. Simulation Configuration

Density of D2D pairs(λ_d)	$10\lambda_B$
packet size（B）	$100\,bits$
Time slot duration (Δt)	$1\,ms$
D2D Transmit power(p_D)	$23\,dBm$
The power of the additive white Gaussian noise	$-104\,dBm$
Transmission range between D2D-TX and D2D-RX（ r_d ）	$25\,m$
SINR threshold（ ξ_0^{th} ）	$0dB$
CU buffer capacity（ $L_{\max}$ ）	$10\,kpackets$

Receiver sensitivity for BS(ρ_{BS})	-80 dBm
Target bit error rate	0.001

Fig. 3(a) plots the mean queuing length versus Poisson arrival rate for different pass loss exponent and $\lambda_B = 3BS / km^2$. It can be seen that the numerical results basically coincide with the simulation results and with the rise of λ, the average queue length increase until λ=10 $kpackets / s$ and then the curve tend to be stable. This is because as more data incoming queue, queue length is more close to full. Moreover, the increase of pass-loss exponent steepens the curve and the queue length reaches saturation quickly.

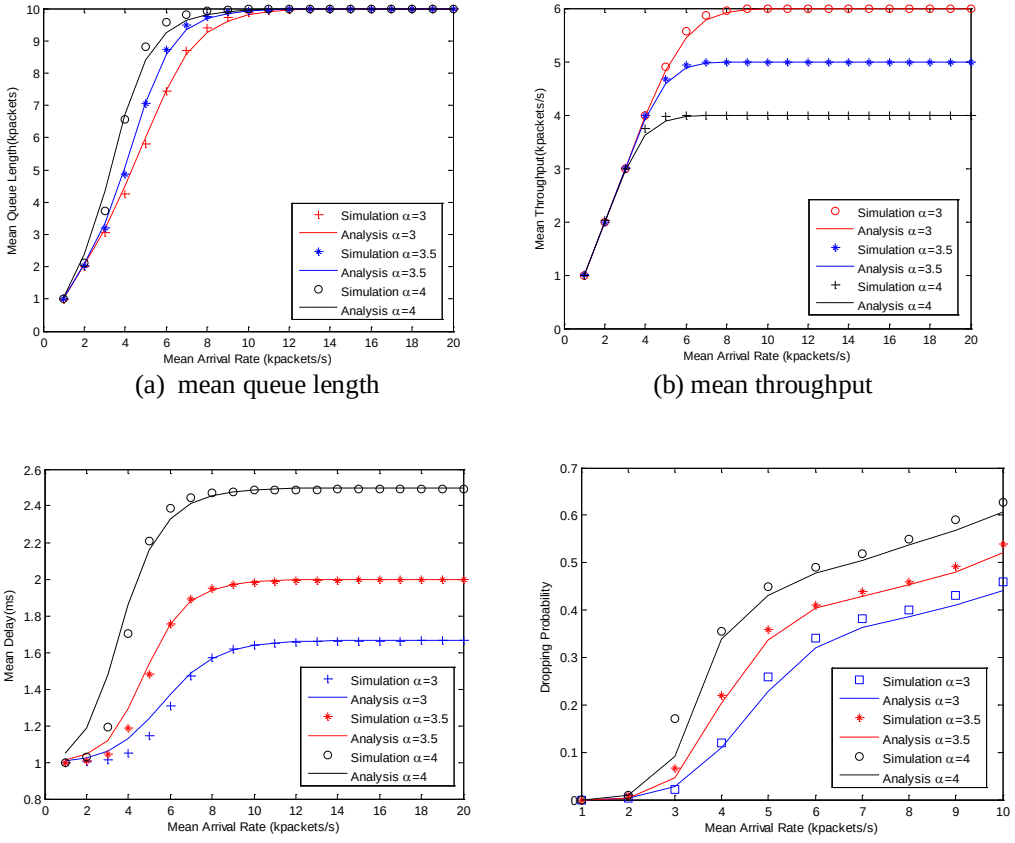

(a) mean queue length (b) mean throughput

(c) mean delay (d) dropping probability

Fig. 3. The CU performance parameters versus packet arrival rate under different α

Fig. 3(b) plots the mean throughput performance of the typical cellular user versus Poisson arrival rate for different pass loss exponent. The mean throughput increases with the packet arrival rate and reaches the maximum transmission capacity when the arrival rate reaches 10 $kpackets / s$. This is because that the data packets in the queue can be sent within a time slot while the arrival rate is relatively low. Thus, the throughput increases rapidly by increasing arrival rate. However, when the arrival rate is higher and exceeds the maximum transmission capacity, the increasing arrival rate only leads to increasing dropping probability. Accordingly, the increasing tendency of curve becomes flat and the arrival packets exceed the

buffer capacity are discarded. Furthermore, with the increase of pass loss exponent, the average throughput decrease and the mean performance of CU shows a downward trend. This is due to the fact that the transmission rate is reduced when SINR of the cellular link decreases. This results in more packets stay in the buffer and average throughput decreases. The numerical analysis and simulation result are perfectly match.

Fig. 3(c) plots mean delay performance of the typical cellular user versus Poisson arrival rate for different pass-loss exponent. The same as **Fig. 3(a)** and **Fig. 3(b)**, the general trends are that the mean delay firstly increase when arrival rate increases, and then the curve tend to very gently when λ is close to the mean sending rate. The mean delay reaches the maximum value firstly and then keeps steady according to Little's Law. This is because that when the amount of arrival data become larger, the packets in the queue cannot be sent within a time slot and mean delay become longer. However, the mean delay holds steady due to the buffer overflows. On the other side, the transmission rate decreases with the increase of pass-loss exponent. There are more packets in the queue and the mean delay is longer. It can be seen that the numerical results basically coincide with the simulation results and with the rise of λ.

Fig. 3(d) plots dropping probability performance of the typical cellular user versus Poisson arrival rate for different pass-loss exponent. Because of the limit of user buffer, when the data packets accumulated in the queue exceed the transmission capacity, the subsequent data packets make dropping probability increase. Moreover, the sending rate decreases with the increase of α, which leads to longer waiting time and larger dropping probability.

Fig. 4 shows the performance parameters versus packet arrival rate when BS density varies. We set α=3 and $L_{\max} = 10kpackets$. the theoretical results are close to the simulation results with all these parameter settings. In **Fig. 4(a)**, with the increase of mean arrival rate, mean queue length is much steeper to reach the maximum capacity with larger BS density. Because of $\lambda_d = 10\lambda_B$, the more interference from D2D users, the slower transmission rate of packets of CU. Sparse BS model relatively slows down the rate of reaching saturation. **Fig. 4(b)** and **Fig. 4(c)** show that the dense BS area($\lambda_B = 5BS/km^2$) results in lower mean throughput and larger mean delay compared with the performance of $\lambda_B = 1BS/km^2$ and $\lambda_B = 3BS/km^2$. The reason is that when the received interference of CU is higher, the more packets cannot be sent within a time slot. Thus, packets need to wait longer time to be transmitted as shown in **Fig. 4(c).**

Fig. 4(d) shows the dropping probability with vary of packet arrival rate under different λ_B. As discussed ahead, the dropping probability caused by overflow which related to mean arrival rate and transmission ability under the fixed buffer size. When $\lambda_B = 1BS/km^2$, dropping probability remains at a relatively low level under the mean arrival rate is 5kpackets/s and the curve rises slowly with the increase of arrival rate. When $\lambda_B = 5BS/km^2$, dropping probability reaches 0.3 and increases rapidly. It illustrates that high dropping probability happens in the dense urban area due to the low sending rate. It is observed that the simulation results are very close to the theoretical results.

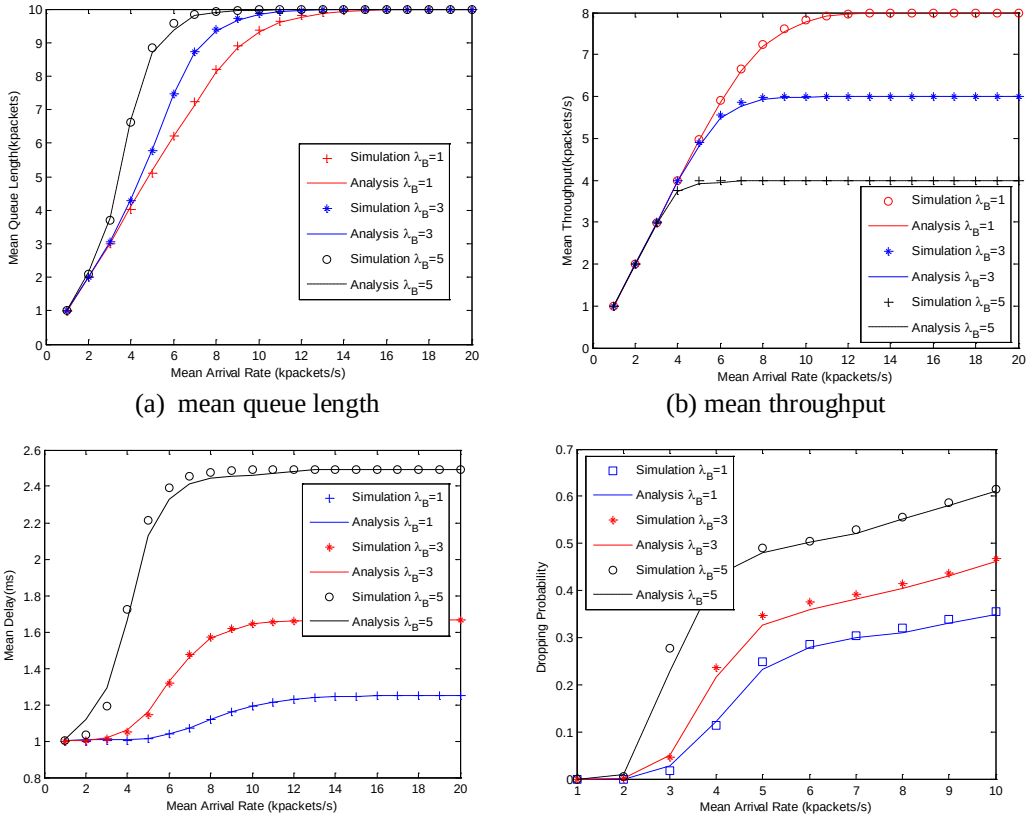

(a) mean queue length (b) mean throughput

(c) mean delay (d) dropping probability

Fig. 4. The CU performance parameters versus packet arrival rate under different λ_B

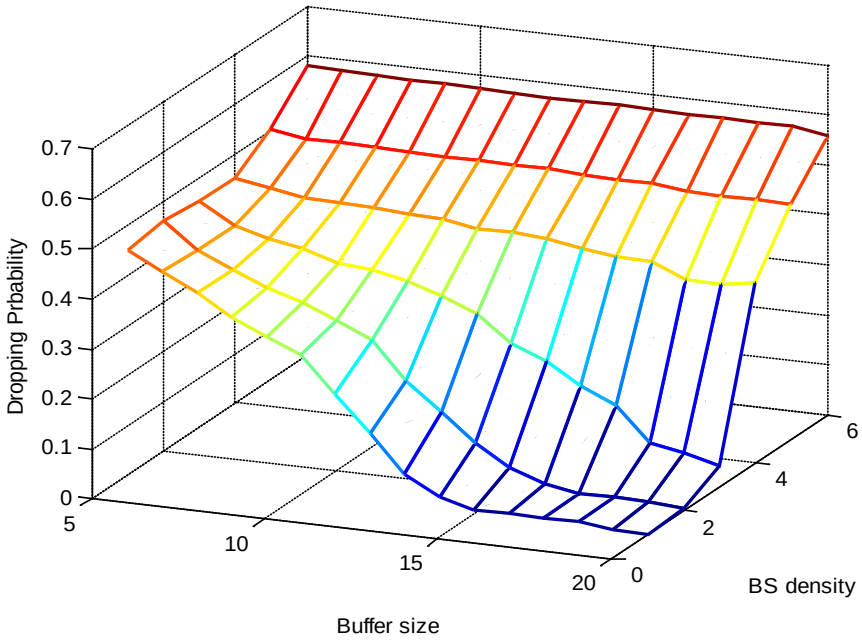

Fig. 5. The CU dropping probability vary under different buffer size and BS density

Fig. 5 illustrates three-dimensional diagram of mean dropping probability under the varying of CU queue buffer size and BS density. We set λ=5*kpackets* / *s* and α=3. From **Fig. 5**, we can see mean dropping probability correspondingly declines with the increase of buffer size and ascends with the increase of BS density. When BS density is lower, buffer size of less than 15 brings about low drop rate. The reason is that high sending rate ensures transmission of most of data packets in the queue and the relatively larger buffer decreases overflow. When BS density is up to $4BS/km^2$, the more interference from D2D users cause over 30% dropping probability even if buffer size is 20. This is because that lower SINR of cellular user leads to mass of data packets backlogging in the queue. So long as the parameters of the cellular user are appropriate, the dropping probability could maintain lower value.

Fig. 6 compares the mean delay between limited-buffer model and infinite buffer model. We set $\alpha = 3, 3.5, 4$ and the buffer size of limited-buffer model is 10kpackets. It is observed that the mean delay of limited-buffer model greatly less than infinite buffer model. Mean delay stabilizes around 2.4ms under $\alpha = 4$ and $L_{\max} = 10$, while mean delay reaches 22ms under $\alpha = 4$ and $L_{\max} = \infty$. Obviously, it is not conforming to the requirement of delay in wireless communications and the limited-buffer model we presented is actually more accurate as well as much more tractable.

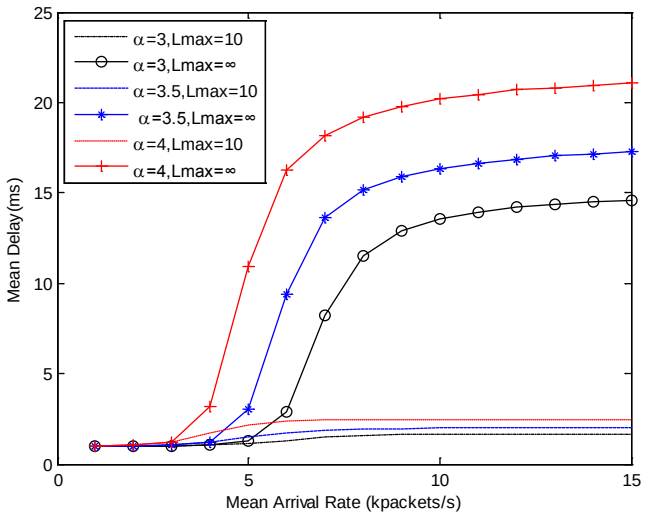

Fig. 6. The mean delay versus packet arrival rate under $L_{\max} = 10$ and $L_{\max} = \infty$

5. Conclusion

In this paper, we present spatiotemporal modeling analysis of cellular user in underlay D2D communication. Stochastic geometry is used to model users spatial distribution accounting for mutual interference which usually assume backlogged traffic queues. Queuing theory develops a dynamic traffic model with adaptive transmission rate, which captures the time evolution of user buffer. The transmission rates of cellular user are constrained by the probability that the SINR of cellular user in a predefined interval, which is derived by stochastic geometry, based model. The probability that the SINR of cellular user in a predefined interval, which constrains the corresponding transmission rate of cellular user. In

the derivation, Embedded Markov chain is introduced to depict the stationary distribution of cellular user queue status. The expressions of performance metrics in terms of mean queue length, mean throughput, mean delay and mean dropping probability are obtained, respectively. Simulation results show the validity and rationality of the theoretical analysis under different interference conditions.

References

[1] K. Doppler, M. Rinne, C. Wijting, C. B. Ribeiro, and K. Hugl, "Device-to-device communication as an underlay to LTE-advanced networks," *IEEE Communications Magazine*, vol. 47, no. 12, pp. 42–49, Dec. 2009. Article (CrossRef Link).

[2] A. Asadi, Q. Wang, and V. Mancuso, ''A survey on device-to-device communication in cellular networks," *IEEE Communications Surveys & Tutorials*, vol. 16, no. 4, pp. 1801–1819, Nov. 2014. Article (CrossRef Link).

[3] P. Mach, Z. Becvar, and T. Vanek, "In-band device-to-device communication in OFDMA cellular networks: A survey and challenges," *IEEE Communications Surveys & Tutorials*, vol. 17, no. 4, pp. 1885–1922, 4th Quart., 2015. Article (CrossRef Link).

[4] J. Liu, N. Kato, J. Ma, and N. Kadowaki, "Device-to-device communication in LTE-advanced networks: A survey," *IEEE Communications Surveys & Tutorials*, vol. 17, no. 4, pp. 1923–1940, 4th Quart., 2015. Article (CrossRef Link).

[5] C. Gao, J. Tang, X. Sheng, W. Zhang, S. Zou, and M. Guizani, "Enabling green wireless networking with device-to-device links: A joint optimization approach," *IEEE Transactions on Wireless Communications* , vol. 15, no. 4, pp. 2770–2779, Apr. 2016. Article (CrossRef Link).

[6] M. Ali, S. Qaisar, M. Naeem, and S. Mumtaz, "Energy efficient resource allocation in D2D-assisted heterogeneous networks with relays," *IEEE Access*, vol. 4, pp. 4902–4911, Sep. 2016. Article (CrossRef Link).

[7] G. Yu, L. Xu, D. Feng, R. Yin, G. Y. Li, and Y. Jiang, "Joint mode selection and resource allocation for device-to-device communications," *IEEE Transactions on Communications*, vol. 62, no. 11, pp. 3814–3824, Nov. 2014. Article (CrossRef Link).

[8] Li, Xiaoshuai, et al, "Joint power control and proportional fair scheduling for D2D communication underlaying cellular networks," in *Proc. of IEEE International Conference on Signal Processing*, 2017. Article (CrossRef Link).

[9] J. Andrews, F. Baccelli, and R. Ganti, "A tractable approach to coverage and rate in cellular networks," *IEEE Transactions on Communications*, vol. 59, no. 11,pp. 3122–3134, Nov. 2011. Article (CrossRef Link).

[10] H. ElSawy, E. Hossain, and M. Haenggi, "Stochastic geometry for modeling, analysis, and design of multi-tier and cognitive cellular wireless networks: A survey," *IEEE Communications Surveys & Tutorials*, vol. 15, no. 3, pp. 996–1019, 2013. Article (CrossRef Link).

[11] M. Haenggi, *Stochastic Geometry for Wireless Networks*, Cambridge, U.K.: Cambridge Univ. Press, 2012. Article (CrossRef Link).

[12] Esmat, Haitham H., M. M. Elmesalawy, and I. I. Ibrahim, "Joint channel selection and optimal power allocation for multi-cell D2D communications underlaying cellular networks," *Iet Communications*, vol. 11, no. 5, pp. 746-755, 2017. Article (CrossRef Link) \.

[13] Guo, Jing, et al, "Device-to-Device Communication Underlaying a Finite Cellular Network Region," *IEEE Transactions on Wireless Communications*, vol. 16, no. 1, pp. 332–347, 2017.Article (CrossRef Link).

[14] Lin, Xingqin, J. G. Andrews, and A. Ghosh, "Spectrum Sharing for Device-to-Device Communication in Cellular Networks," *IEEE Transactions on Wireless Communications*, vol. 13, no. 12, pp. 6727-6740, 2014. Article (CrossRef Link).

[15] Elsawy, Hesham, E. Hossain, and M. S. Alouini, "Analytical Modeling of Mode Selection and Power Control for Underlay D2D Communication in Cellular Networks," *IEEE Transactions on Communications*, vol. 62, no. 11, pp. 4147–4161, 2014. Article (CrossRef Link) .

[16] Fowler, Scott, et al, "Analysis of vehicular wireless channel communication via queueing theory model," in *Proc. of IEEE International Conference on Communication*, pp. 1736-1741,2014. Article (CrossRef Link) .
[17] Lall, S., A. S. Alfa, and B. T. Maharaj, "The role of queueing theory in the design and analysis of wireless sensor networks: An insight," in *Proc. of IEEE International Conference on Industrial Informatics*, pp.1191-1194,2017. Article (CrossRef Link).
[18] Abd-Elmagid, Mohamed A., T. Elbatt, and K. G. Seddik, "On the role of finite queues in cooperative cognitive radio networks with energy harvesting," in *Proc. of IEEE International Conference on Computing, NETWORKING and Communications*, 2017. Article (CrossRef Link).
[19] Liang, Guangjun, et al, "Performance Analysis of Buffer-Aided Relaying System Based on Data and Energy Coupling Queuing Model for Cooperative Communication Networks," *Wireless Communications & Mobile Computing* 2017(2017):1-14. Article (CrossRef Link).
[20] Lei, Lei, et al, "Performance Analysis of Device-to-Device Communications with Dynamic Interference Using Stochastic Petri Nets," *IEEE Transactions on Wireless Communications s*, vol. 12, no. 12, pp. 6121-6141, 2013. Article (CrossRef Link).
[21] Mou, Xiaohan, L. Lei, and Z. Zhong, "Performance Analysis of Resource Allocation Schemes in Device-to-Device Communications with Bursty Traffic," in *Proc. of IEEE International Conference on Information Science & Applications* , pp.1-4, 2014. Article (CrossRef Link).
[22] Shaqfeh, Mohammad, et al, "Maximizing Expected Achievable Rates for Block-Fading Buffer-Aided Relay Channels," *IEEE Transactions on Wireless Communications*, vol. 15, no. 9, pp. 5919–5931, 2017. Article (CrossRef Link).
[23] Jia, Xiangdong, et al, "Outage performance analysis for buffer-aided relay system over non-identical Rayleigh fading channels," *Iet Communications*, vol. 9, no.15, pp. 1842–1851, 2017. Article (CrossRef Link).
[22]A. Doufexi, S. Armour, M. Butler, A. Nix, D. Bull, J. McGeehan, and P. Karlsson, "A comparison of the HIPERLAN/2 and ieee 802.11a wireless LAN standards," *IEEE Communications Magazine*, vol. 40, no. 5, pp. 172–180, May 2002. Article (CrossRef Link).
[24] Zheng, Qiang, et al, "Dynamic Performance Analysis of Uplink Transmission in Cluster-Based Heterogeneous Vehicular Networks," *IEEE Transactions on Vehicular Technology*, vol. 64, no.12, pp. 5584-5595, 2017. Article (CrossRef Link).
[25] M. Ni, L. Zheng, F. Tong, J. Pan, and L. Cai, "A geometrical based throughput bound analysis for device-to-device communications in cellular networks," *IEEE Journal on Selected Areas in Communications*, vol. 33, no. 1, pp. 100–110, Jan. 2015. Article (CrossRef Link).
[26] N. Lee, X. Lin, J. G. Andrews, and R. W. Heath, "Power control for D2D underlaid cellular networks: Modeling, algorithms, and analysis," *IEEE Journal on Selected Areas in Communications* , vol. 33, no. 1, pp. 1–13, Jan. 2015. Article (CrossRef Link).

Jianfang Xin received the master degree in Telecommunication Engineering from the Taiyuan University of Technology (TYUT), China, in 2008. She is currently working toward the doctor degree in Communication and Information System from the Nanjing University of Posts & Telecommunications (NUPT). His research interests include resource allocation for wireless communication, resource allocation for D2D communication.

Qi Zhu (Corresponding Author)received the bachelor and master degree in radio engineering from Nanjing University of Posts & Telecommunications (NUPT), China, in 1986 and 1989, respectively. She is now a full-time professor in the School of Telecommunication and Information Engineering of NUPT. Her research interests focus on technology of next generation communication, broadband wireless access, OFDM, channel and source coding, dynamic allocation of radio resources.

GuangJun Liang received the master degree in Telecommunication Engineering from the Taiyuan University of Technology (TYUT), China, in 2008. He is currently working toward the doctor degree in Communication and Information System from the Nanjing University of Posts & Telecommunications (NUPT). His research interests include resource allocation for wireless communication, OFDMA systems and relaying, resource allocation for Mobile Networking.

Tianjiao Zhang received the bachelor degree in Telecommunication Engineering from the Nanjing University of Posts & Telecommunications (NUPT), China, in 2013. He is currently working toward the doctor degree in Communication and Information System from the Nanjing University of Posts & Telecommunications (NUPT).His research interests include optimization for wireless communication, physical resource allocation for V2V Networking.

Su Zhao received the bachelor in radio engineering from Nanjing University of Posts & Telecommunications (NUPT), China, in 2005. She is now vice President of the School of Telecommunication and Information Engineering of NUPT. Her research interests focus on mobile communication and wireless technology, MIMO.